*[Earth's Future]*

Supporting Information for

# Projecting future fire regimes in semiarid systems of inland northwestern U.S.: interactions among climate change, vegetation productivity, and fuel dynamics

[1,2]Jianning Ren, [2]Erin J. Hanan, [3]John T. Abatzoglou, [3]Crystal A. Kolden, [4]Christina (Naomi) L. Tague, [5]Maureen C. Kennedy, [1]Mingliang Liu, [1]Jennifer C. Adam

1 Department of Civil & Environmental Engineering, Washington State University, 99163, Pullman, USA

2 Department of Natural Resources and Environmental Sciences, University of Nevada, Reno, 89501, Reno, USA

3 Management of Complex Systems, University of California, Merced, 95344, Merced, USA

4 Bren School of Environmental Science & Management, University of California, Santa Barbara, 93106, Santa Barbara, USA

5School of Interdisciplinary Arts and Sciences, Division of Sciences and Mathematics, University of Washington, Tacoma, 98402, Tacoma, USA

## Contents of this file



## Introduction

The first part of supplementary material includes a detailed description of WMFire and fire effect model. The second part includes results of RHESSys model calibration and WMFire validation. The third part are supplementary figures to support results and discussion.

**Text S1. Model descriptions**

S1.1 Fire spread model

WMFire is a stochastic fire-spread model designed to be coupled with RHESSys (Kennedy et al., 2017). It takes output variables from RHESSys and uses them to predict fire spread. Because it is an intermediate-complexity stochastic model, WMFire is not designed to predict the perimeters and timing of individual fires. Instead, the model can be used to predict aggregate spatial and temporal characteristics of fire spread across basins over time (i.e., the fire regime). A successful ignition occurs when there is an ignition source on the landscape, and it successfully starts a wildfire. The successful start of fire (Pi(l,d), Eqn 1) is calculated from the probabilities associate with litter load and relative deficit (Pi(l)) and Pi(d), respectively), where deficit is calculated as 1-ET/PET (here, we use relative deficit as a surrogate for fuel aridity). The probability of a successful spread (Ps(l,d,S,w)) is calculated based on the probabilities associate with litter load (l), relative deficit (d), topographic slope (S) and the orientation of spread relative to wind direction (W), giving Ps(l), Ps(d), Ps(S), and Ps(w), respectively (Eqn 2). The probability of spread (Ps) increases with increasing fuel load and relative deficit, is highest in the direction of wind, increases in the uphill direction, and decreases in the downhill direction. After a successful ignition, WMFire tests the orthogonal neighbors of that patch against the probability of spread to determine if there is a successful spread. WMFire model has demonstrated accuracy in the Santa Fe (New Mexico) and HJ Andrews (Oregon) watersheds (Kennedy et al., 2017).

$$Pi\,(l,d)=Pi\,(l)\times Pi\,(d) \qquad \text{Equation (S1)}$$

$$Ps\,(l,d,S,w)=Ps\,(l)\times Ps\,(d)\times Ps\,(w)\times Ps\,(S) \qquad \text{Equation (S2)}$$

S1.2 Fire effects model

The fire effects model is built to match the complexity of the coupled RHESSys-WMFire model (Bart et al., 2020). The fire effects model uses the probability of spread (Ps) as an index of fire intensity but also accounts for canopy structure, which links fire intensity and spread with fire severity. Fire consumes C in the litter and coarse woody debris (CWD) pools based on the CONSUME model (an empirical model developed using statistical relationships derived from measured woody fuel consumption data; Ottmar et al., 1993). Passive crown fire is spread from the understory to the overstory. For the understory, Ps is a proxy for fire intensity, and the fire-caused mortality is a function of intensity (currently it is a 1:1 linear relationship, but can be changed to account for different landscapes). For the overstory, mortality and consumption of fuel are based on how much litter and understory fuel are consumed. There is also a set of parameters to account for the understory height threshold, overstory height threshold, and functional form representing the relationship between mortality and consumption. The fuel that is not consumed moves into the litter and CWD pools.

**Text S2. Model parameterization**

We used a Monte Carlo approach to calibrate six groundwater-related parameters: saturated hydraulic conductivity (Ksat), decay of Ksat with depth (m), air-entry pressure ($\phi ae$), pore size index (b), bypass flow to deeper groundwater stores (gw1) and groundwater drainage rates to the stream (gw2). We selected the best parameter set for Trail Creek by comparing observed and modeled streamflow using the Nash-Sutcliffe efficiency metric (NSE), R2 for the correlation between daily observed and modeled flow, and percent error in annual flow estimates as well MODIS ET and NPP (Mu et al., 2011). The Monthly NSE is 0.94 with a percent

error of 2.6 for calibration period. The model estimates ET and NPP in a reasonable range. A detailed description of hydrologic calibration is described by Ren et al., (2021).

The fire spread model WMFire has previously been shown to replicate expected spatial patterns of fire spread for a wildfire in the Pacific Northwest (Kennedy et al., 2017) and fire regime characteristics for two different watersheds with contrasting historical fire regimes (LANDFIRE, Rollins, 2009). The model is robust to applications in both historically low severity frequent-fire regimes in the southwest and mixed to high severity infrequent fire regimes in the Pacific Northwest. We selected three criteria (spatial distribution of fire spread, fire seasonality, fire return interval (FRI) to validate the fire spread model against LANDFIRE estimates for Trail Creek. Spatial distribution and seasonality of fire were not sensitive to ignition rates and agreed with LANDFIRE estimates. FRI, on the other hand, was sensitive to ignition rates. We adjusted ignition rates according to the size of Trail Creek, which enabled RHESSys-WMFire to simulate spatial variation in FRIs that agreed with LANDFIRE estimates. A detailed description of WMFire model calibration is described in (Hanan et al., 2021).

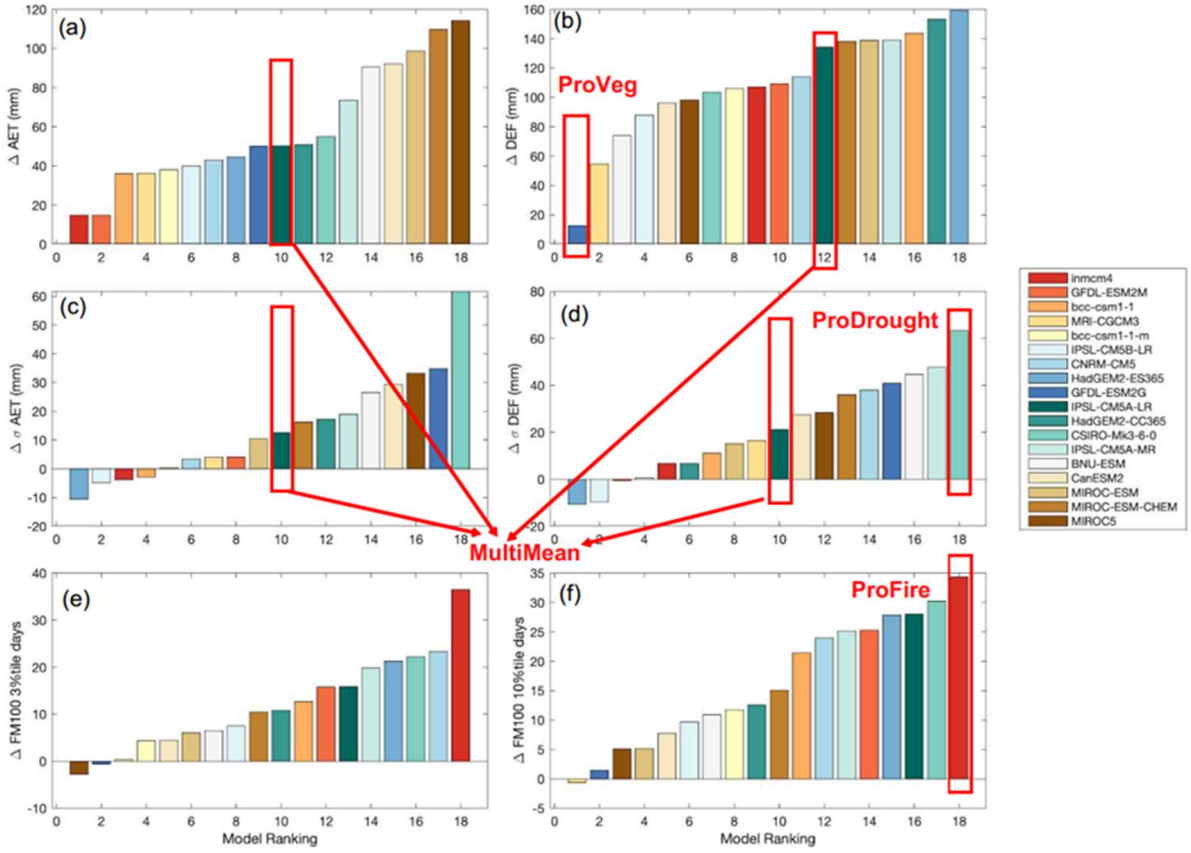


**Figure S1.** The ranking of fire-related climate change variables among GCM models for Trail Creek according to the future greenhouse gas emission RCP8.5 scenarios. These variables include the 1971 – 2000 vs. 2040 – 2069 changes in the monthly mean of a) actual evaporation (ΔAET) and b) water deficit (ΔDEF), the standard deviation of monthly c) AET (σAET) and d) DEF (σDEF); annual number of days per year where 100-hour dead fuel moisture is below the historical (1971 – 2000) value for the e) 3rd percentile and f) 10th percentile. ProDrought had the

largest increase in the standard deviation of DEF from the historical (1971 – 2000) period; this represents a storyline where drought would be promoted. ProVeg had the smallest increase in the mean of DEF, which would increase productivity and limit fire; and ProFire had significant variability in fire-related metrics; MultiMean is the GCM model that was closest to the multi-model mean.

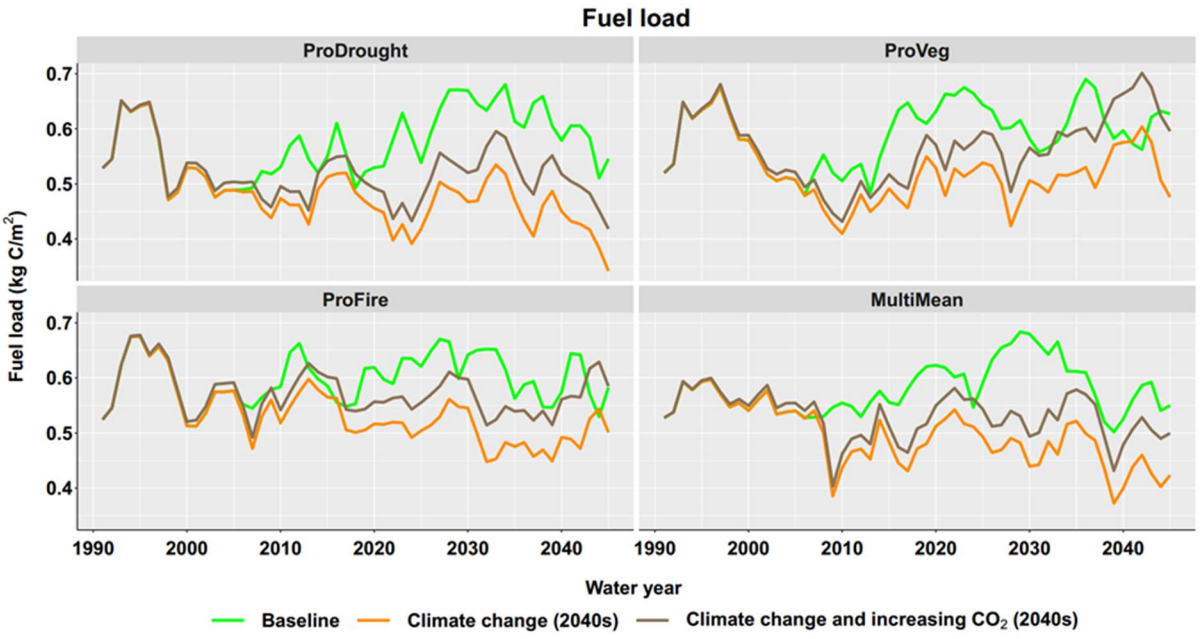


**Figure S2.** Basin scale fuel load (i.e., litter carbon) response to climate change and atmospheric CO2 fertilization effect under four different GCMs scenarios for 2040s. Baseline scenario used historical climate data for the future scenario spin-up. These scenarios are without fire model on.

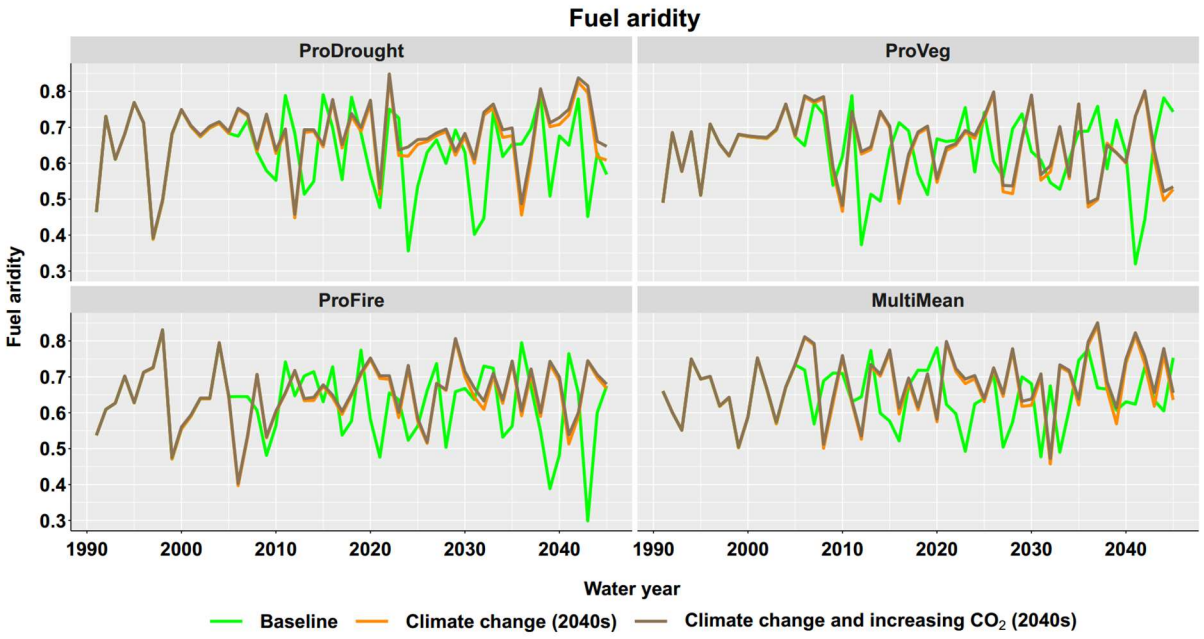


**Figure S3.** Basin scale fuel aridity response to climate change and atmospheric CO2 fertilization effect under four different GCMs scenarios for 2040s. These scenarios are without fire model on.

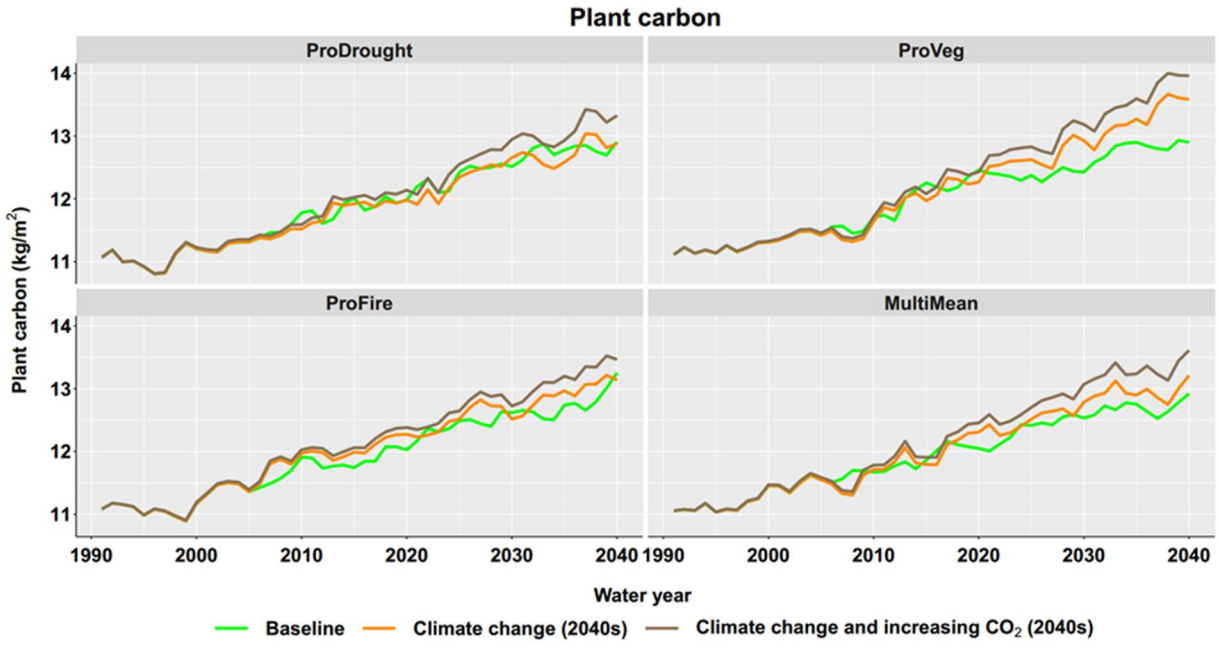


**Figure S4.** Basin scale plant carbon response to climate change and atmospheric CO2 fertilization effect under four different GCMs scenarios for 2040s. These scenarios are without fire model on.

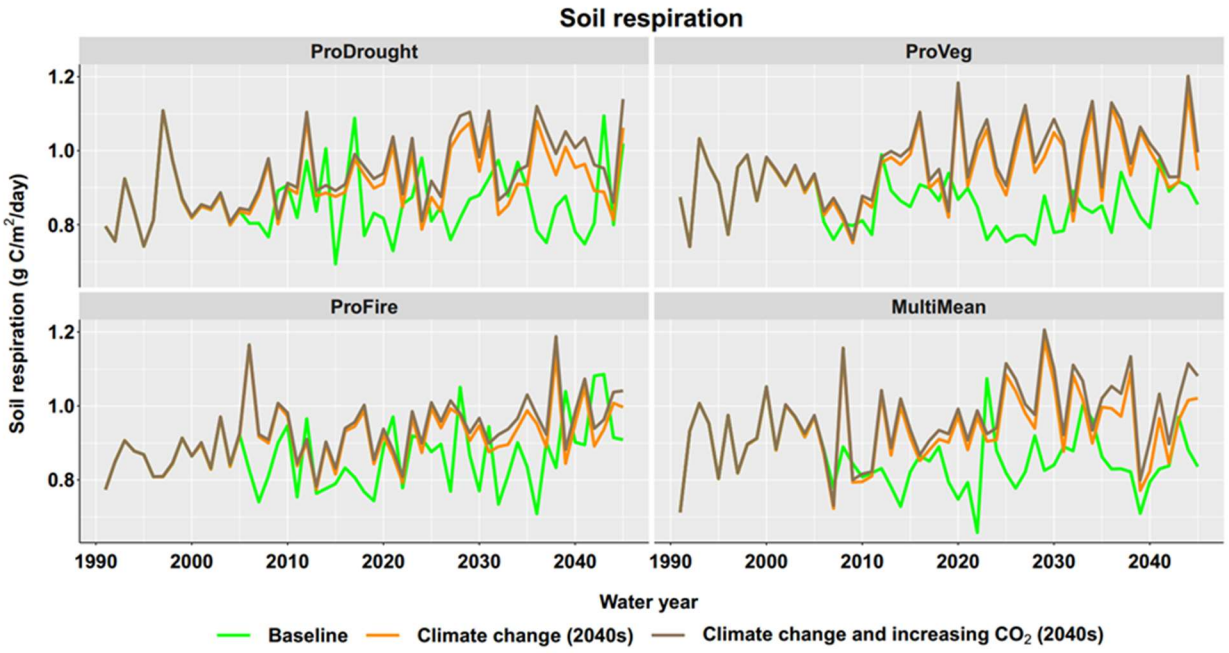


**Figure S5.** Basin scale soil respiration response to climate change and atmospheric CO2 fertilization effect under four different GCMs scenarios for 2040s. These scenarios are without fire model on.

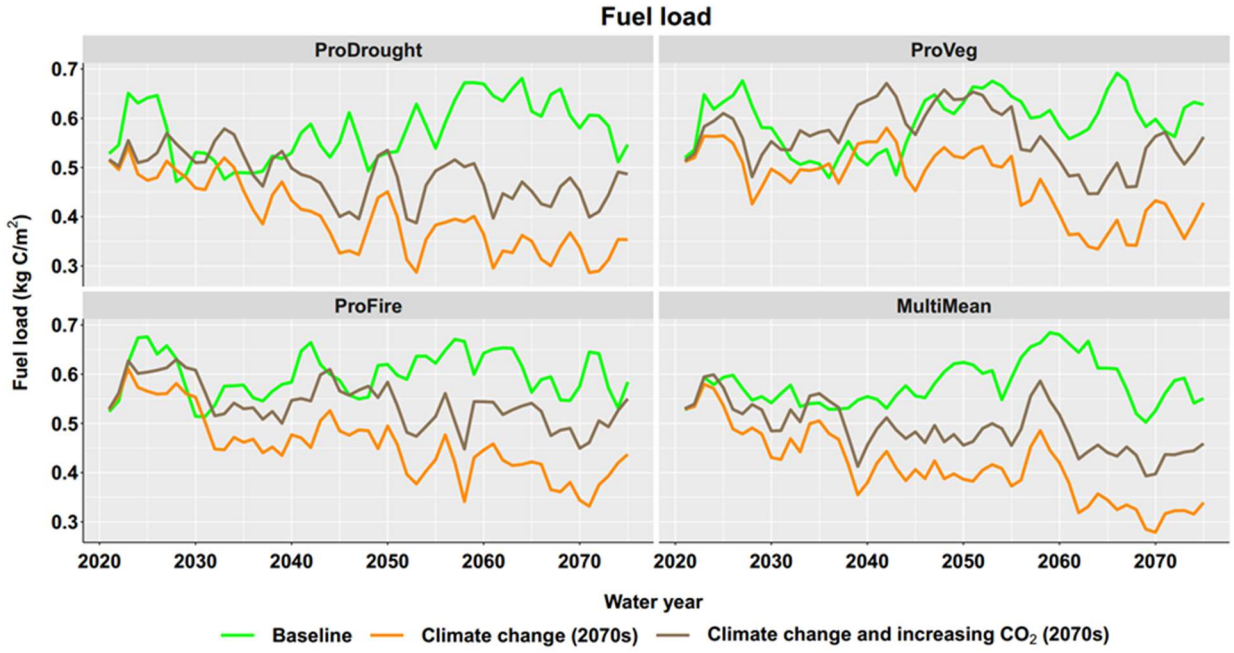


**Figure S6.** Basin scale fuel load (i.e., litter carbon) response to climate change and atmospheric CO2 fertilization effect under four different GCMs scenarios for 2070s. These scenarios are without fire model on.

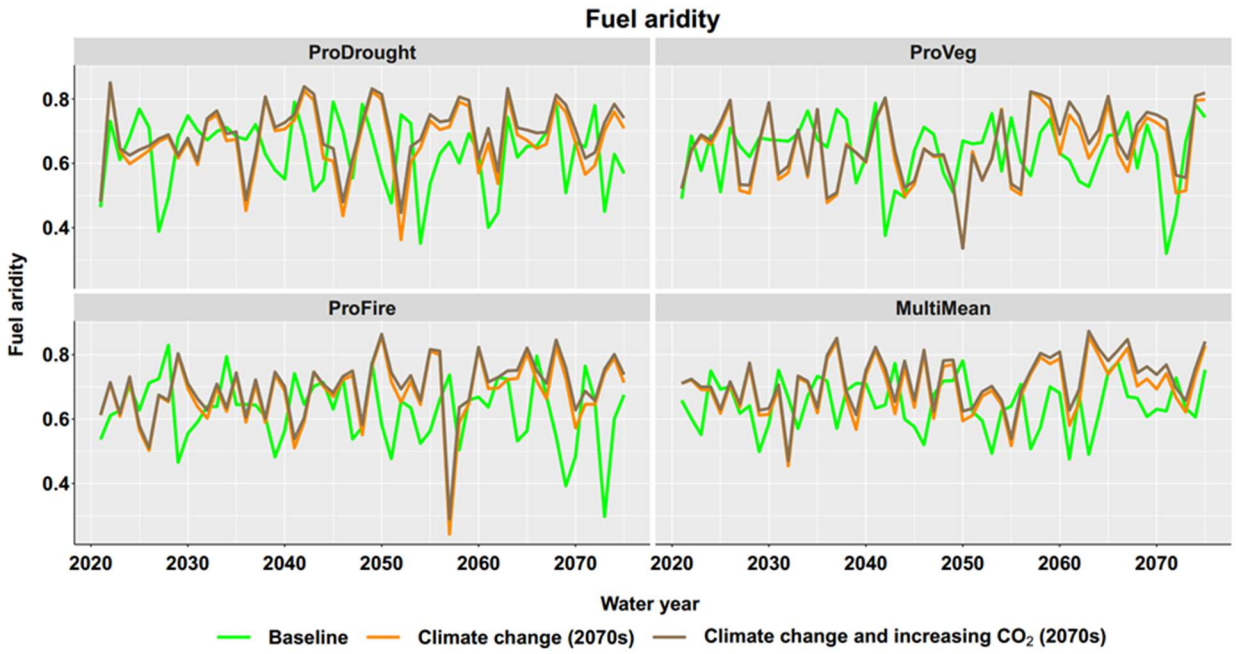


**Figure S7.** Basin scale fuel aridity response to climate change and atmospheric CO2 fertilization effect under four different GCMs scenarios for 2070s. These scenarios are without fire model on.

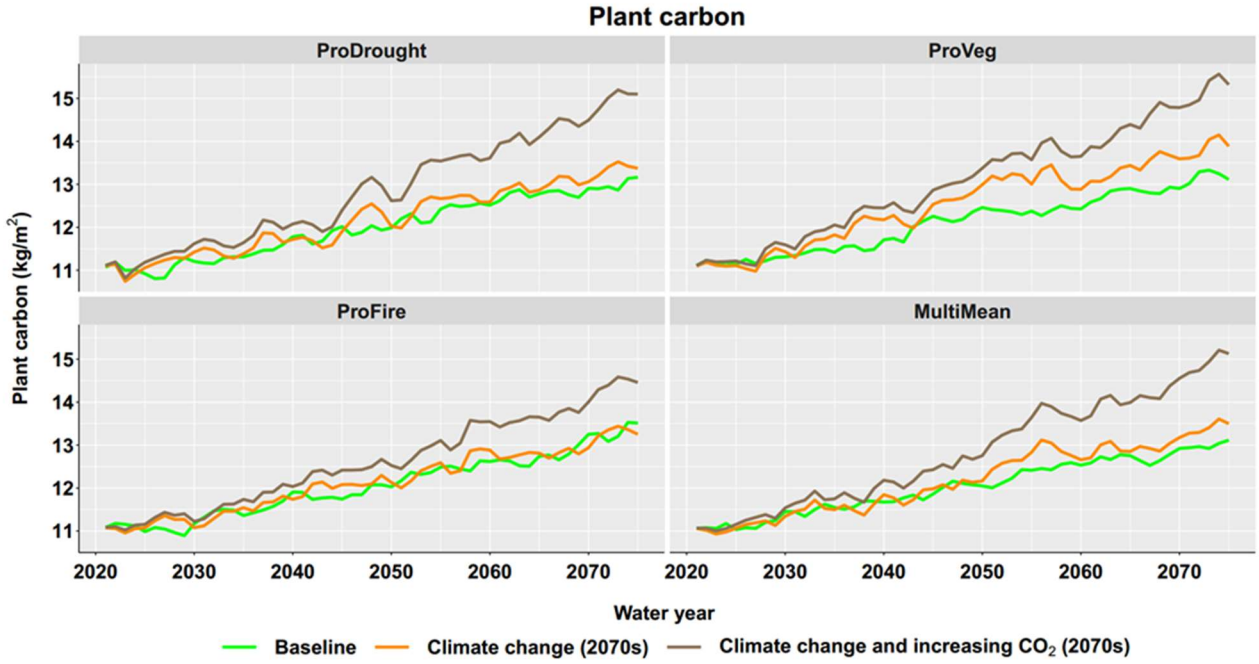


**Figure S8.** Basin scale plant carbon response to climate change and atmospheric CO2 fertilization effect under four different GCMs scenarios for 2070s. These scenarios are without fire model on.

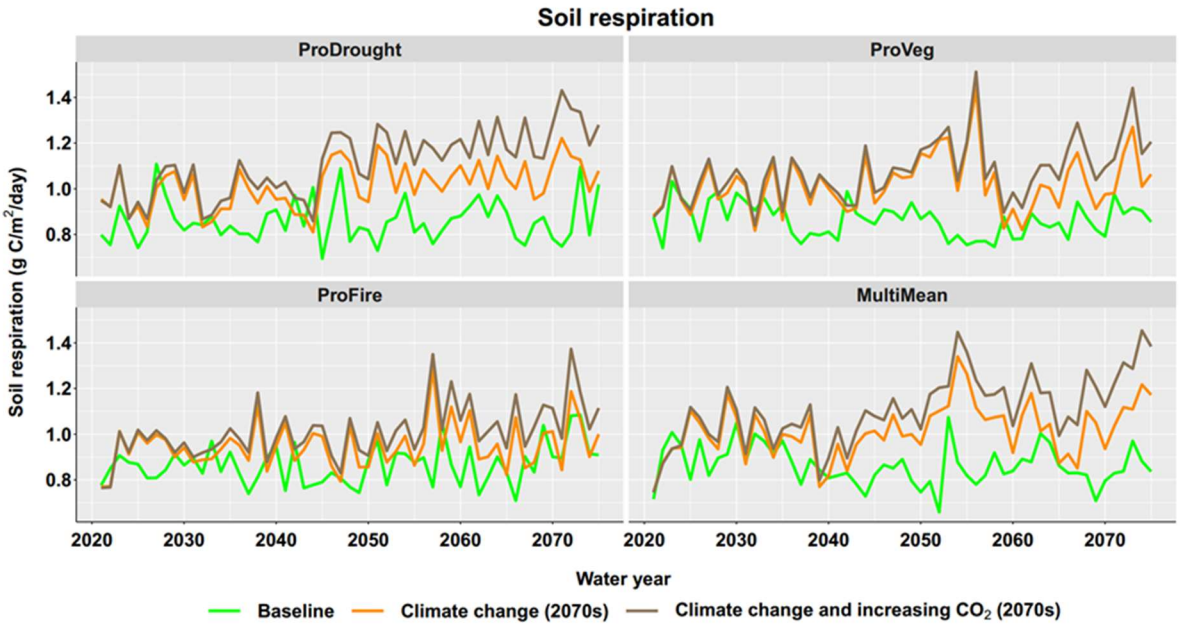


**Figure S9.** Basin scale soil respiration response to climate change and atmospheric CO2 fertilization effect under four different GCMs scenarios for 2070s. These scenarios are without fire model on.

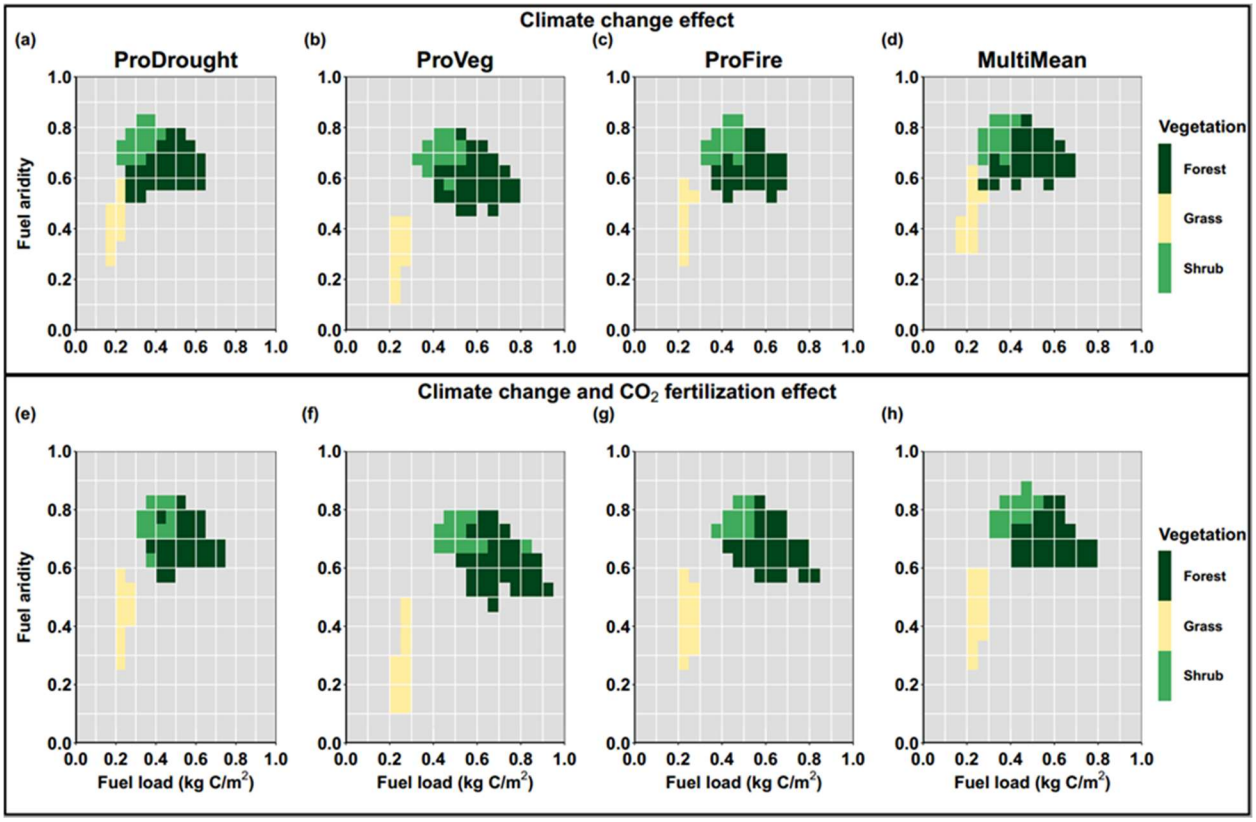

**Figure S10**. Relationships among fuel load, fuel aridity, and vegetation distribution under various climate change and atmospheric CO2 fertilization effect scenarios in 2040s. Data are bind with 0.05 window length for both fuel load and fuel aridity, and the value of each bin is the median number of vegetation types. Panel (a), (b), (c), and (d) show the only climate change effect and panel (e), (f), (g), and (h) show the overall effect (both climate change and CO2 fertilization effect).

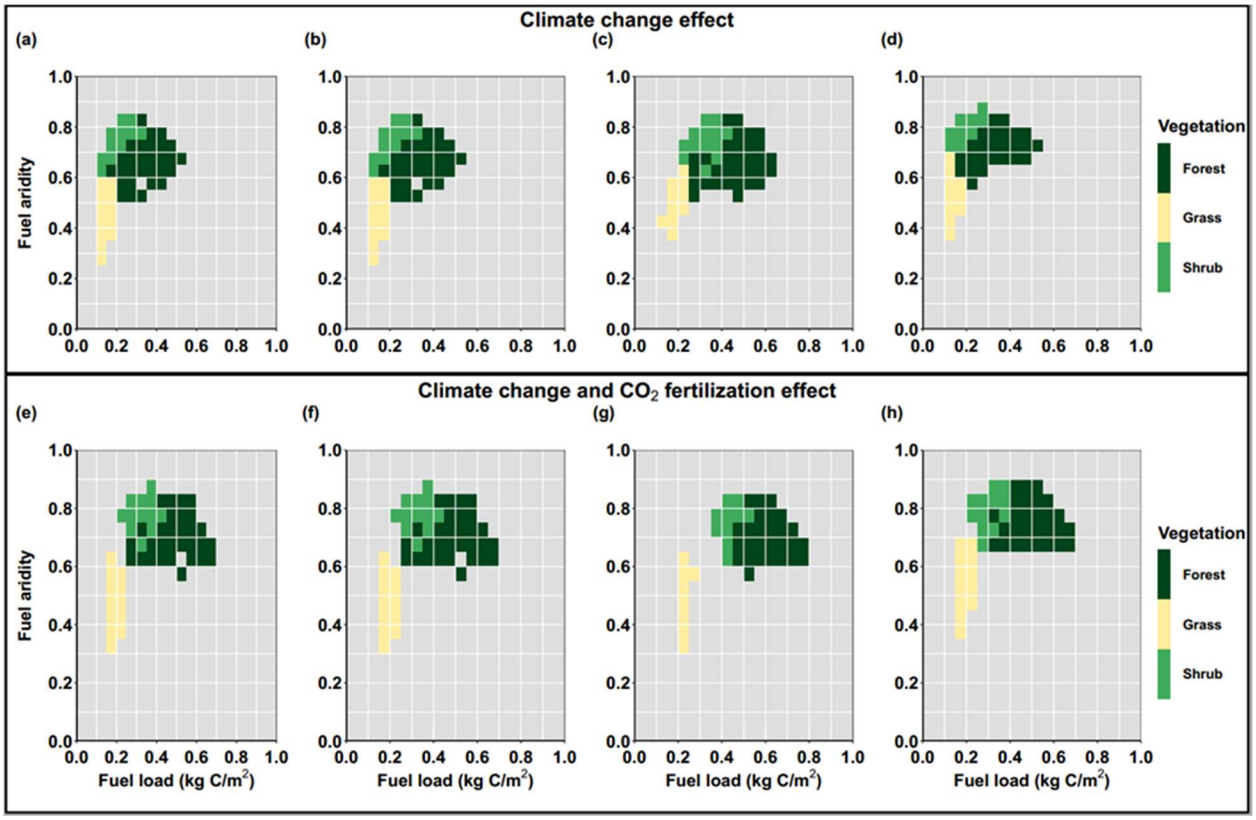


**Figure S11.** Relationships among fuel load, fuel aridity, and vegetation distribution under various climate change and atmospheric CO2 fertilization effect scenarios in 2070s. Data are bind with 0.05 window length for both fuel load and fuel aridity, and the value of each bin is the median number of vegetation types. Panel (a), (b), (c), and (d) show the only climate change effect and panel (e), (f), (g), and (h) show the overall effect (both climate change and CO2 fertilization effect).

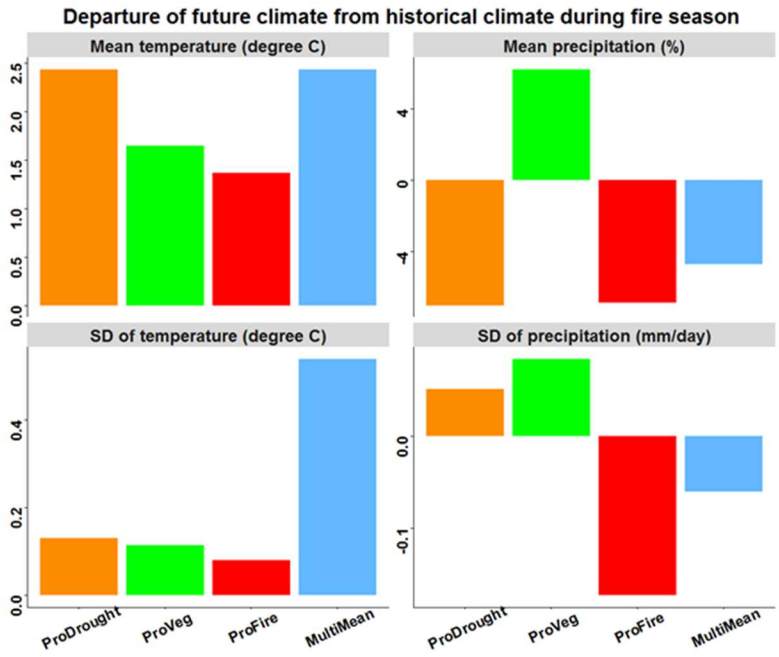


**Figure S12**. Differences between future climate (2006 - 2060) and historical climate (1991 - 2005) during the fire season (May -September). The top panels are the differences in the annual mean, and the bottom are the differences in the standard deviation (SD).

**References:**

Bart, R. R., Kennedy, M. C., Tague, C. L., & McKenzie, D. (2020). Integrating fire effects on vegetation carbon cycling within an ecohydrologic model. Ecological Modelling, 416, 108880. https://doi.org/10.1016/j.ecolmodel.2019.108880

Hanan, E. J., Ren, J., Tague, C. L., Kolden, C. A., Abatzoglou, J. T., Bart, R. R., et al. (2021). How climate change and fire exclusion drive wildfire regimes at actionable scales. Environmental Research Letters, 16(2), 024051. https://doi.org/10.1088/1748-9326/abd78e

Kennedy, M. C., McKenzie, D., Tague, C., & Dugger, A. L. (2017). Balancing uncertainty and complexity to incorporate fire spread in an eco-hydrological model. International Journal of Wildland Fire, 26(8), 706. https://doi.org/10.1071/WF16169

Mu, Q., Zhao, M., & Running, S. W. (2011). Improvements to a MODIS global terrestrial evapotranspiration algorithm. Remote Sensing of Environment, 115(8), 1781–1800. https://doi.org/10.1016/j.rse.2011.02.019

Ottmar, R. D., Burns, M. F., Hall, J. N., & Hanson, A. D. (1993). CONSUME: users guide. (No. PNW-GTR-304). Portland, OR: U.S. Department of Agriculture, Forest Service, Pacific Northwest Research Station. https://doi.org/10.2737/PNW-GTR-304

Ren, J., Adam, J. C., Hicke, J. A., Hanan, E. J., Tague, C. L., Liu, M., et al. (2021). How does water yield respond to mountain pine beetle infestation in a semiarid forest? Hydrology and Earth System Sciences, 25(9), 4681–4699. https://doi.org/10.5194/hess-25-4681-2021

Rollins, M. G. (2009). LANDFIRE: a nationally consistent vegetation, wildland fire, and fuel assessment. International Journal of Wildland Fire, 18(3), 235–249. https://doi.org/10.1071/WF08088